



Suppression of current fluctuations in a crossed $E \times B$ field system for low-voltage plasma immersion treatment

I. Levchenko, M. Keidar, K. Ostrikov, and M. Y. Yu

Citation: *Journal of Applied Physics* **99**, 013301 (2006); doi: 10.1063/1.2136416

View online: <http://dx.doi.org/10.1063/1.2136416>

View Table of Contents: <http://scitation.aip.org/content/aip/journal/jap/99/1?ver=pdfcov>

Published by the [AIP Publishing](#)

Articles you may be interested in

[Two-dimensional simulation of ac-driven microplasmas confined to 100 – 300 \$\mu\$ m diameter cylindrical microcavities in dielectric barrier devices](#)

J. Appl. Phys. **100**, 123302 (2006); 10.1063/1.2398024

[Current transport studies of ZnO/p-Si heterostructures grown by plasma immersion ion implantation and deposition](#)

Appl. Phys. Lett. **88**, 132104 (2006); 10.1063/1.2190444

[Density and production of NH and NH₂ in an Ar – N₂ expanding plasma jet](#)

J. Appl. Phys. **98**, 093301 (2005); 10.1063/1.2123371

[Characterization of remote inductively coupled CH₄ – N₂ plasma for carbon nitride thin-film deposition](#)

J. Appl. Phys. **98**, 043308 (2005); 10.1063/1.2032617

[Comparison between radical- and energetic ion-induced growth of SiC_xN_y films in plasma immersion ion implantation and deposition](#)

J. Appl. Phys. **96**, 7681 (2004); 10.1063/1.1812587



AIP | Journal of Applied Physics

Journal of Applied Physics is pleased to announce **André Anders** as its new Editor-in-Chief

Suppression of current fluctuations in a crossed $\mathbf{E} \times \mathbf{B}$ field system for low-voltage plasma immersion treatment

I. Levchenko^{a)}*School of Physics, University of Sydney, Sydney NSW 2006, Australia*

M. Keidar

*Department of Aerospace Engineering, University of Michigan, Ann Arbor, Michigan 48109*K. Ostrikov^{b)}*School of Physics, University of Sydney, Sydney NSW 2006, Australia*

M. Y. Yu

Institute for Theoretical Physics I, Ruhr University Bochum, Bochum 44780, Germany

(Received 18 April 2005; accepted 19 October 2005; published online 3 January 2006)

Plasma transport in a hybrid dc vacuum arc plasma source for ion deposition and plasma immersion treatment is considered. It is found that external crossed electric and magnetic fields near the substrate can significantly reduce the relative amplitude of ion current fluctuations \bar{I}_f at the substrate surface. In particular, \bar{I}_f decreases with the applied magnetic field when the bias voltage exceeds 300 V, thus allowing one to reduce the deviations from the rated process parameters. This phenomenon can be attributed to an interaction between the metal-plasma jet from the arc source and the discharge plasma in the crossed fields. © 2006 American Institute of Physics.

[DOI: [10.1063/1.2136416](https://doi.org/10.1063/1.2136416)]

I. INTRODUCTION

The hybrid ion deposition/plasma immersion ion treatment (ID/PIIT) is a promising approach for improving the surface properties of mechanical parts by enhancing their chemical stability and wear resistance.¹⁻³ Typically, the ID/PIIT process involves two main stages, repeated at a rate of a few hertz to several kilohertz. In the ion deposition stage, a coating is deposited on a substrate by an ion flux extracted from a metal or carbon plasma generated in a vacuum arc plasma source (VAPS).⁴ In the plasma immersion treatment stage, a negative bias voltage is applied repetitively to the substrate immersed in the plasma, and an ion flux is extracted from the plasma and accelerated through the near-substrate plasma sheath. The application of the negative bias enables one to treat the growing coating by an ion flux with controllable kinetic energy. This improves the surface layer and coating structure through heating and activation of the adsorbed atoms on the substrate surface during film growth.^{5,6} Both high-⁷ and low-⁸ voltage processes have been effectively used for treating various functional materials. Low-voltage treatment (in the range of several kilovolts) can result in a notable improvement of the coating hardness.^{1,9} Increase of hardness can also be achieved at several tens of kilovolts.¹⁰

Pulsed VAPSs have several drawbacks. The deposition occurs only in the discharge run (the “arc off” phases are wasted for the purpose of deposition), resulting in lower

deposition rates than that in dc VAPS systems. Moreover, the quality of films synthesized in pulsed systems is often compromised by unwanted contaminant deposition between the arc pulses.¹¹ Besides, in a pulsed system the desired parameters for film synthesis cannot be maintained during the entire deposition cycle since the required ratio of the ion/reactive gas densities [e.g., titanium ions Ti^+ , Ti^{2+} , and Ti^{3+} and hydrocarbon radicals and/or atomic nitrogen for synthesis of titanium nitride (TiN), titanium carbide (TiC), or complex titanium carbonitride ($\text{Ti}_x\text{C}_{1-x}\text{N}$) coatings] is disrupted during the “off” phase. Thus, continuously operating dc VAPS systems are more promising for fabrication of dense films with controlled elemental composition, structural, and other properties.

However, violent current fluctuations that can greatly reduce the process efficiency frequently occur in continuously operating dc VAPS systems. The fluctuation level depends on the regime of the VAPS operation¹² as well as the cathode spot dynamics.¹³ The movement of the cathode spots can be controlled by external focusing magnetic field \mathbf{B}_f .^{14,15} Even though the application of \mathbf{B}_f can improve VAPS stability, the current fluctuation level in the system can still remain high.

We introduce here a hybrid ID/PIIT system comprising a dc vacuum arc metal plasma source and crossed magnetic and electric fields near the substrate. A prototype of this facility designed for low-voltage plasma treatment has been tested.¹⁶ In this device, no pulsed bias is applied, and the treatment is achieved by simultaneous deposition of metal ions and bombardment of the growing film with ions extracted from a gas discharge in crossed $\mathbf{E} \times \mathbf{B}$ fields sustained around the cylindrical substrate, where \mathbf{E} and \mathbf{B} are the near-substrate electric and magnetic fields. Thus, the process is conducted in a steady-state regime. Time-averaged current-

^{a)}Permanent address: National Aerospace University, Kharkov, Ukraine.

^{b)}Also with the Plasma Sources and Applications Center, NIE, Nanyang Technological University, 637616 Singapore. Author to whom all correspondence should be addressed; electronic mail: K.Ostrikov@physics.usyd.edu.au

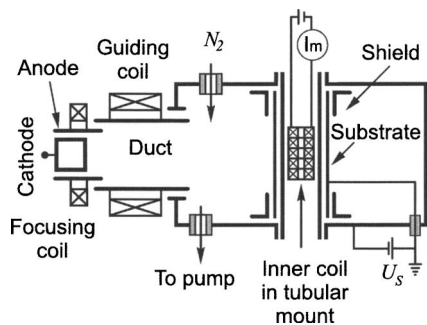


FIG. 1. Experimental setup.

voltage characteristics of a similar system with crossed $\mathbf{E} \times \mathbf{B}$ fields have been previously reported.¹⁷ Recently, it has been shown that magnetic field can affect the thickness of the near-substrate sheath.¹⁸ The parameters of various systems without¹⁹ and with²⁰ the transverse magnetic field have been investigated in the regime when the substrate bias pulses were applied at a rate of several hertz.

Hybrid systems with a plasma jet as well as crossed $\mathbf{E} \times \mathbf{B}$ fields are often characterized by a high level of near-substrate current fluctuations. Unfortunately, at present neither effective remedy nor systematic study of the enhanced fluctuations exist. Here we propose an efficient method for reducing the relative amplitude of ion current fluctuations in a hybrid ID/PIIT system featuring a dc vacuum arc metal plasma source and near-substrate crossed magnetic and electric fields. It is shown that if the near-substrate electric field is strong enough, the application of crossed $\mathbf{E} \times \mathbf{B}$ fields results in a substantial suppression of the relative amplitude of ion current fluctuations and can lead to an improvement of the stability of plasma processing.

II. EXPERIMENTAL SETUP

A schematic diagram of the experimental setup is shown in Fig. 1. The hybrid facility consists of a vacuum chamber, a cylindrical substrate, an inner coil, and a VAPS. A tubular mount with the inner coil and the cylindrical substrate, negatively biased relative to the grounded chamber walls, is installed axially in the vacuum chamber. The substrate and inner coil are housed in a water-cooled cylindrical vacuum chamber with a volume of 0.25 m^3 (inner diameter 0.55 m and length 1.0 m). The inner coil is 100 mm in diameter and total length of 200 mm, located in the tubular mount. Inside the coil, a core of 40 mm diameter and 200 mm length made of a soft steel (magnetic permeability $\mu \approx 1000$) is inserted in order to increase the magnetic field. The internal space of the tubular mount is not evacuated, thus allowing us to cool the coil by a continuous air flow. The cylindrical substrate of 500 mm length and 120 mm diameter, made from a nonmagnetic austenitic stainless steel (18% chromium and 10% nickel) tube, is installed concentrically on the tubular mount. Insulation made of several layers of a thin asbestos tape is fitted between the grounded tubular mount walls and the cylindrical substrate to prevent gas breakdown in the gap between them. The upper and lower sections of the substrate surface are covered with tubular metal shields to avoid arcing in the areas where the magnetic field lines intersect the

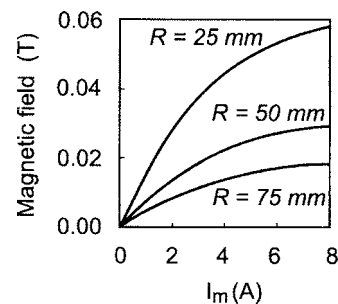


FIG. 2. Dependence of the magnetic field strength on magnetic coil current I_m with distance R (on the coil axis of symmetry) from the substrate surface as a parameter.

substrate surface. The shields are insulated and maintained at a floating potential. The dependence of the magnetic field strength on the magnetic-coil current I_m with the distance from the substrate R as a parameter is shown in Fig. 2.

A metal plasma jet is produced by a direct-current VAPS with a cathode of 50 mm diameter and 50 mm length and a grounded anode of 120 mm diameter. The cathode is made of titanium. The vacuum arc is triggered by a high-voltage pulse generated by the igniting circuit. The source operates at a nominal current of 100 A. The cathode spots are retained on the cathode face surface by the magnetic field generated by a focusing coil, installed above the anode. The VAPS is mounted on the flange of a plasma duct of 180 mm diameter and 260 mm length. The exit flange of the plasma duct is attached to the vacuum chamber port. A guiding coil on the duct sustains a guiding magnetic field \mathbf{B}_g , along which the plasma is transported to the chamber. The distance between the duct exit and the substrate axis is 250 mm.

An automated gas feed system maintains the nitrogen pressure p_0 at $\sim 1 \text{ Pa}$. This pressure is most appropriate for deposition of titanium-based films in such devices. The pressure is controlled by a combination of an electromagnetic valve, a mechanical backing pump, and a high-vacuum oil pump. The pressure is measured with a thermocouple vacuum gauge and two ionization gauges.

Two independent dc power supply units are used to maintain a voltage from 0 to 0.5 kV between the grounded chamber walls and the substrate (with maximum current 20 A), and a voltage from 0 to 100 V between the cathode and anode of the VAPS (with maximum current 110 A). The stabilized power supply units operate at the transformation frequency of 16 kHz; the amplitude of ripples does not exceed 1.0% of the nominal rectified current for the VAPS supply unit and 0.5% for the bias supply unit. The slope of the current-voltage characteristics of the power supply units does not exceed 0.1 V/A for the VAPS supply unit (in the current range from 60 to 110 A) and 0.07 V/A for the bias supply unit (in the current range 0 to 10 A). The current, current fluctuations, voltage and pressure are recorded by an automated data acquisition system (DAS) connected to a computer via an analog-to-digital converter (ADC). The digital sampling rate of the ADC is 10 kHz, and the analog bandwidth of the DAS is approximately 1 MHz.

Measurements were made for three values (90, 100, and 110 A) of the VAPS current I_a covering the range of stable

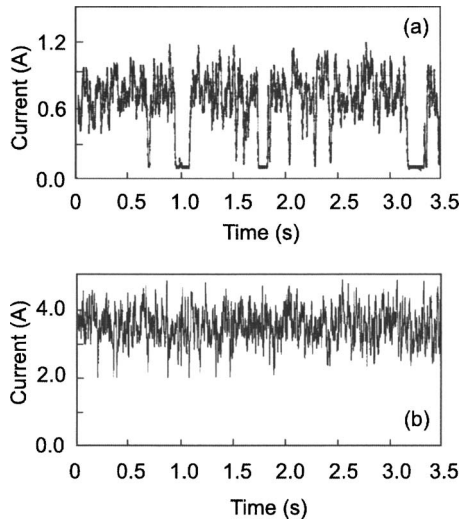


FIG. 3. Oscillograms of the ion current at the substrate surface for $I_a = 100$ A and $U_s = 500$ V, for (a) $I_m = 0$ and (b) $I_m = 5$ A.

operation of the VAPS. Bias voltages from 100 to 500 V provide stable deposition without arcing to the substrate.²¹ On the other hand, in the range of magnetic coil currents from 0 to 7 A, magnetic fields from 0 to 0.1 T are generated. Under these conditions, the plasma electrons are strongly magnetized in the vicinity of the substrate surface.

III. RESULTS

Oscillograms of the ion current at the substrate surface taken for the VAPS current $I_a = 100$ A, bias voltages $U_s = 500$ V, and magnetic coil currents $I_m = 0$ A and $I_m = 5$ A are shown in Fig. 3. One can see that without the magnetic field the current fluctuations can reach a value which is the same as the mean current. Strong effects by the fluctuations on the plasma immersion treatment process can thus be expected. On the other hand, Fig. 3(b) shows that the application of a magnetic field can significantly reduce the fluctuations. The mean period (~ 0.02 s) of the current fluctuations is unaffected by the magnetic field.

To study the spectral characteristics of the current versus time function, we calculated the discrete probability distribution for the relative amplitude of current fluctuations

$$\bar{I}_f = (|I - \langle I \rangle|) / \langle I \rangle,$$

where I and $\langle I \rangle$ are the actual and mean currents, respectively. The discrete probability distribution is obtained from the recorded oscillograms as follows. The vector file of current values (50 000 data points spanning 5 s) has been scanned. For each data point, i.e., for each time step of 100 μ s, the difference between the actual current and the mean current is determined, with a discreteness set at 1/150 of the mean current. The values are then normalized to 1 according to

$$\alpha \sum_1^n \psi_i = 1, \quad (1)$$

where α is a normalizing coefficient, $n = 150$, and ψ_i is the number of data points having an amplitude in the i th interval

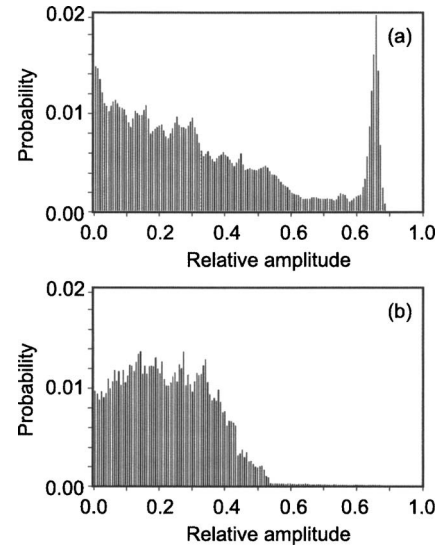


FIG. 4. Distribution of current fluctuation amplitude for the same parameters as in Fig. 3.

of the mean current $\langle I \rangle$, so that the interval width is $\langle I \rangle / n$. In other words, each column in Fig. 4 represents the probability of finding the corresponding fluctuation level (the random part of the current divided by the mean current).

Figure 4 reflects the changes in the spectral characteristics caused by an increase of the magnetic field. From Fig. 4(a), plotted for zero magnetic field one finds that the relative current fluctuations of very large amplitude (85% of the mean) are the most probable. In Fig. 4(b), where a magnetic field is present, one finds a sharp cutoff for relative fluctuation levels exceeding 0.55. In fact, the relative fluctuation level of the ion current is mainly between 15 and 35%, much lower than in the magnetic field-free case. Similar behavior was observed in the entire range (90–110 A) of the vacuum arc current. Thus, when the dc bias voltage exceeds 300 V, one can significantly reduce the relative current amplitude at the substrate \bar{I}_f (in the crossed fields region). With increasing magnetic coil current, \bar{I}_f decreases progressively but saturates at 0.5–0.6. We note that in practical applications the relative amplitude of ion current fluctuations at the substrate determines the severity of the deviation of the deposition conditions from the rated process specifications.

Figure 5 illustrates the dependencies of the maximum relative current amplitude $\bar{I}_{f,m} = (I_{\max} - \langle I \rangle) / \langle I \rangle$, where I_{\max} is the maximum registered current value, on magnetic coil current for different bias voltages and arc current: (a) $I_a = 90$ A and (b) 110 A. Figure 6 shows $\bar{I}_{f,m}$ versus bias voltage at different magnetic coil and arc currents: (a) $I_a = 90$ A and (b) 110 A. From the figures one can see that $\bar{I}_{f,m}$ decreases weakly as the bias voltage changes from 100 to 300 V. However, when the voltage exceeds 300 V, the maximum relative current amplitude appears to be much lower. Interestingly, the magnetic field strength does not appreciably affect the above results. When $\mathbf{B}_0 = 0$, the bias voltage does not affect the amplitude of the relative current fluctuations.

We can therefore conclude that by applying a magnetic field, one can shift the most frequent oscillations from $0.85I_s$

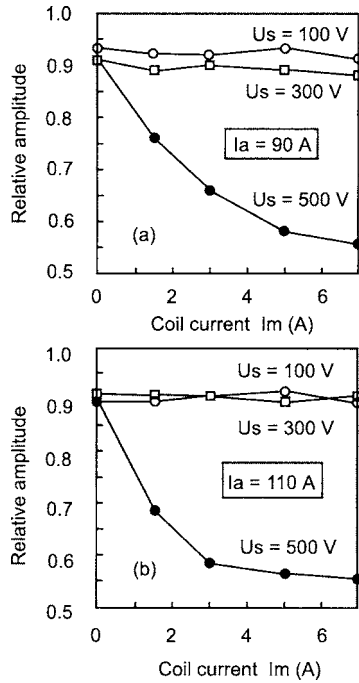


FIG. 5. Dependence of the maximum relative amplitude of the current fluctuation on magnetic coil current I_m with bias voltage U_s and arc current I_a as parameters.

to $0.25I_s$, and decrease the maximum relative amplitude from $0.85I_s$ to $0.55I_s$. Figure 7 presents the dependence of the most frequent (i.e., most probable) relative amplitude of current fluctuations on the magnetic coil current for different VAPS currents at a bias voltage of 500 V (Fig. 7). The most probable relative amplitude decreases smoothly with the coil

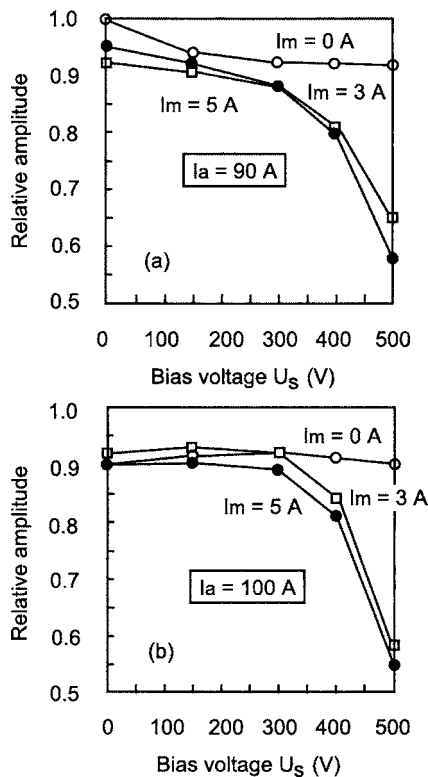


FIG. 6. Same as in Fig. 5 vs bias voltage U_s with I_m and I_a as parameters.

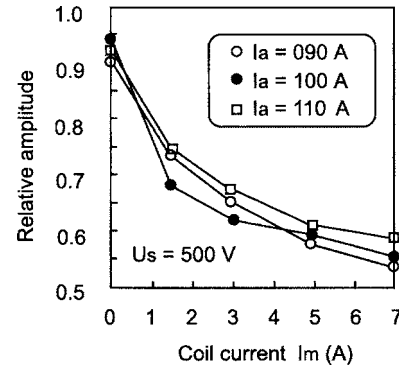


FIG. 7. Dependence of the most probable relative amplitude on magnetic coil current I_m with I_a as a parameter.

current and reaches 0.1–0.2 when the latter approaches 7 A, i.e., at $B=0.06$ T, at 25 mm from the substrate surface. At moderate magnetic fields ($I_m=3$ A) this value approaches 0.3. In its entire range of 90–110 A, the VAPS current does not appreciably affect the relative amplitude of the most frequent fluctuation level.

IV. DISCUSSION

The large-amplitude low-frequency ion current fluctuations in plasma immersion treatment facilities using a VAPS are intimately related to the (metal) plasma production, which occurs mainly in the cathode spots.²² In our experiments the duration of the cathode spots existence²³ is much shorter than the fluctuation period. Thus the observed current fluctuations can be attributed to the spot movement around the cathode surface rather than to the spot generation/quenching processes. Due to specific vacuum source geometry (Fig. 1), the ions from the plasma produced in the spot can deposit directly onto the anode surface when the spots migrate over the lateral (cylindrical) surface facing the gap between the cathode and the anode. When the spots move around the cathode face periphery (closer to the anode), the plasma flux at the plasma duct exit decreases. Thus, the spot movement can produce large-amplitude, low-frequency ion current oscillations. When the arc current is sufficiently large, several spots can exist simultaneously, causing a stochastic pattern of current fluctuations. These fluctuations have a frequency of approximately several tens of hertz, as can be seen in Fig. 2 (the fluctuation period is ~ 0.02 s). It should be noted that these fluctuations do not have their origin in the auxiliary circuits, since the rectification of a three-phase line power produces a higher ripple frequency of approximately $n \times 100$ Hz, typically 300 Hz for the three-phase double-wave rectification. Besides, the recorded fluctuations have an essentially stochastic pattern and are not correlated with the regular oscillations in the power supply circuit.

Our results show that the relative amplitude of current fluctuations is drastically reduced when the magnetic field is applied at the substrate. To explain the results, we now examine the processes occurring in the plasma device with crossed electric and magnetic fields. In this system, the metal plasma stream generated by the VAPS is driven to the substrate by the external electric field created by the negatively

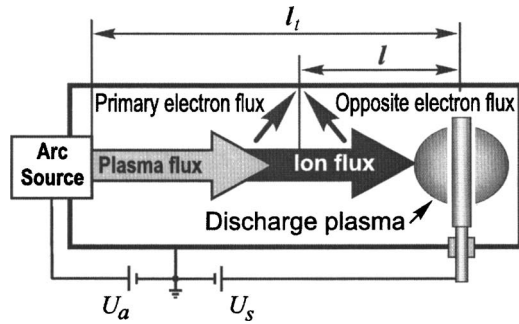


FIG. 8. Schematics of the plasma, ion, and electron fluxes between the VAPS and substrate.

biased substrate. Meanwhile, a toroidal glow-discharge (GD) plasma is sustained around the cylindrical substrate when the gas pressure exceeds 0.01 Pa.¹⁷ The substrate is subject to concurrent ion fluxes from the GD and metal plasmas.¹⁶ Thus, the total current increases, as can be seen in Fig. 3. Therefore, the natural way to explain the current increase is to assume that the pulsating arc current is imposed upon the GD current, and hence the relative amplitude of the substrate current fluctuations decreases.

To verify this assumption, we have measured the substrate current versus I_m at two pressures (0.01 and 1.0 Pa) without the arc source. It is found that the GD cannot be initiated at pressures $p_0 \leq 0.01$ Pa. At $p_0 = 1.0$ Pa, the GD is initiated when the magnetic coil current I_m exceeds 0.6 A. When I_m exceeds 2 A, the GD ion current saturates at $I_S \approx 1.5$ and 2.5 A for dc biases of 400 and 500 V, respectively. Since the GD ion current is added to the metal plasma current (when the VAPS is in operation), the total current to the substrate increases appreciably with the magnetic field, as can be seen by comparing Figs. 3(a) and 3(b). One can thus conclude that the superposition of the metal plasma and glow discharge currents is a cause for the decrease of the current fluctuation level in a low magnetic field (up to $I_m = 2$ A). Since the GD ion current saturates at $I_m = 2$ A, further amplitude decrease cannot be explained by merely adding the gas and metal ion currents, and we propose another possible mechanism.

Let us consider in more detail the transport of the metal plasma to the biased substrate (Fig. 8). When the plasma streams toward the substrate, the electric field accelerates the ion species and slows down the electrons produced by the VAPS (*primary electron flux*). The electrons are also driven by the weak radial electric field and move to the grounded chamber walls. Thus, most of the electrons from the VAPS-generated metal plasma are lost to the grounded walls and do not reach the negatively biased substrate. In the steady state, the quasi-neutral plasma flux to the substrate is mainly sustained by the electron flux produced by background gas ionization near the substrate surface [*opposite electron flux* (OEF)]. It is natural to suppose that the opposite electron flux plays a crucial role in reducing the current oscillations. Let us estimate the transit time τ_e required for the OEF electrons to traverse a given length l .

The classical electron mobility across the magnetic field is

$$\mu_{et} = \frac{m_e v_e}{e B^2}, \quad (2)$$

where m_e is the electron mass, v_e is the electron-neutral collision frequency, and e is the electron charge. The electron velocity across the magnetic field is then

$$V_{et} = \mu_{et} E_t, \quad (3)$$

where E_t is electric field directed to the substrate. Thus, the electron transit time is

$$\tau_e = l/V_{et} = l/\mu_{et} E_t, \quad (4)$$

which after substitution of Eq. (2) into Eq. (4) yields

$$\tau_e = \frac{e l B^2}{m_e v_e E_t}. \quad (5)$$

The electric field is mainly concentrated in a thin sheath at the substrate surface, only a weak electric field from the small voltage drop $U_r = k_r U_s$ is present outside the sheath, where $k_r \ll 1$, and U_s is the dc bias voltage. Taking into account that the current oscillations cannot be smoothed for voltages below 300 V, one can use $k_r = 0.01$, assuming that electrons (from the VAPS) with the energy $\varepsilon_e = 3$ eV (Ref. 3) are mainly decelerated after they have traversed the gap between the arc source and the substrate. Approximating the distance the electrons travel from the near-substrate area (opposite electron flux) as $l = l_r k_r U_s / (2\varepsilon_e)$, where l_t is the distance between the substrate and vacuum arc source ($l_t = 0.3$ m), and taking the electric field outside the sheath as $E_t = 2\varepsilon_e / l_t$, we obtain

$$\tau_e = \frac{e k_r U_s}{m_e v_e} \left(\frac{l_t B}{2\varepsilon_e} \right)^2 \quad (6)$$

for the time required for the OEF electrons to traverse the near-substrate area. Using $v_e = n_a \sigma_a V_e$ for the electron-neutral collision frequency, $p_0 = 1$ Pa for the working gas pressure, $\sigma_a = 10^{-20}$ m² for the electron-neutral collision cross section, $V_e = 10^6$ m/s (3 eV) for the electron thermal velocity, $B = 0.005$ T for the magnetic field (at $I_m = 3$ A, the field measured at a distance of 150 mm from the substrate surface, i.e., between the substrate surface and vacuum arc source), and $U_s = 300$ V for the voltage, the estimated electron transit time is $\tau_e = 0.015$ s. Note that this value is less than the mean period of the measured current fluctuations. On the other hand, for $U_s = 500$ V we have $\tau_e = 0.025$ s, which exceeds the mean period of the current fluctuations τ_{cf} . We emphasize that the electron transit time is less than the period of current fluctuations ($\tau_e < \tau_{cf}$) at $U_s = 300$ V, whereas $\tau_e > \tau_{cf}$ at $U_s = 500$ V.

Under such conditions, the current fluctuations are smoothed as follows. When the plasma production rate transiently increases, the ion flux toward the substrate surface becomes stronger. Meanwhile, OEF electrons drifting from the substrate toward the plasma duct exit tend to compensate the increased ion flux. Within the electron transit time τ_e , most of the increased (i.e., noncompensated or “excessive”) ion flux is deposited onto the chamber walls since the quasineutral plasma moving across the magnetic field is not supported by the opposite electron flux. If the enhanced

plasma generation discontinues before the OEF electrons arrive to the duct exit, the excessive ion flux is dissipated on the walls, and the current fluctuation cannot reach the substrate. On the other hand, if the excessive plasma production still continues when the OEF electrons approach the duct exit, higher-density neutralized plasmas are subject to quite different transport conditions. The prevailing conditions are favorable for the increased plasma flux to reach the substrate sheath. Hence, more intense ion fluxes can be extracted, causing an increase in the substrate current. We can thus conclude that the layer of plasma with magnetized electrons acts as an efficient magnetic shield that impedes the propagation of the plasma plumes ejected in pulses shorter than the time τ_e required for the OEF electrons to traverse the magnetic shield area.

The previous estimates are valid when the time τ_i of ion transit from the plasma duct exit to the substrate surface is much shorter than the electron transit time τ_e and the characteristic time scale of the current fluctuations. Assuming that the energy of Ti^+ ions is 10 eV and taking into account that the ion flux is not magnetized, we have an ion transit time of 5×10^{-5} s, which is much less than the estimated electron transit time.

V. CONCLUSION

Thus, the application of a transverse magnetic field noticeably decreases the relative amplitude of the substrate current fluctuations (from 85% down to 55% for the maximum level, and down to 25% for the most probable level) due to the magnetic shielding effect. When the bias voltage exceeds 300 V, relative amplitudes of the current fluctuations decrease with the magnetic field. However, at dc bias voltages lower than 300 V, application of even strong magnetic fields does not affect the high-amplitude fluctuations. We have also shown that variations in the VAPS current I_a do not noticeably affect the current fluctuation level.

ACKNOWLEDGMENTS

This work was partially supported by the Australian Research Council, the University of Sydney, Lee Kuan Yew Foundation, and the Agency for Science, Technology, and Research.

- ¹A. Anders, *Surf. Coat. Technol.* **93**, 158 (1997).
- ²*Handbook of Plasma Immersion Ion Implantation and Deposition*, edited by A. Anders (Wiley, New York, 2000).
- ³J. M. Schneider, S. Rohde, W. D. Sproul, and A. Matthews, *J. Phys. D* **33**, R173 (2000).
- ⁴J. Rosen, A. Anders, L. Hultman, and J. M. Schneider, *J. Appl. Phys.* **94**, 1414 (2003).
- ⁵I. Levchenko, M. Romanov, O. Baranov, and M. Keidar, *Vacuum* **72**, 335 (2003).
- ⁶K. Ostrikov, *Rev. Mod. Phys.* **77**, 489 (2005).
- ⁷I. G. Brown, X. Godechot, and K. M. Yu, *Appl. Phys. Lett.* **58**, 1392 (1991).
- ⁸S. Mukherjee, J. Chakraborty, S. Gupta, P. M. Raole, P. I. John, K. R. M. Rao, and I. Manna, *Surf. Coat. Technol.* **156**, 103 (2002).
- ⁹R. Günzel, M. Betzl, I. Alphonsa, B. Ganguly, P. I. John, and S. Mukherjee, *Surf. Coat. Technol.* **112**, 307 (1999).
- ¹⁰M. Ueda, L. A. Berni, R. M. Castro, A. F. Beloto, E. Abramof, J. O. Rossi, J. J. Barroso, and C. M. Lepienski, *Surf. Coat. Technol.* **156**, 71 (2002).
- ¹¹D. M. Sanders and A. Anders, *Surf. Coat. Technol.* **133–134**, 78 (2000).
- ¹²B. Juttner, *J. Phys. D* **34**, R103 (2001).
- ¹³B. Juttner and I. Kleberg, *J. Phys. D* **33**, 2025 (2000).
- ¹⁴V. N. Zhitomirsky, R. L. Boxman, and S. J. Goldsmith, *J. Vac. Sci. Technol. A* **13**, 2233 (1995).
- ¹⁵I. I. Beilis, M. Keidar, R. L. Boxman, and S. Goldsmith, *J. Appl. Phys.* **83**, 709 (1998).
- ¹⁶I. Levchenko, M. Romanov, and M. Korobov, *Surf. Coat. Technol.* **184/2–3**, 356 (2004).
- ¹⁷I. Levchenko, M. Romanov, and M. Keidar, *J. Appl. Phys.* **94**, 1408 (2003).
- ¹⁸M. Keidar, O. R. Monteiro, and I. G. Brown, *Appl. Phys. Lett.* **76**, 3002 (2000).
- ¹⁹I. G. Brown, O. R. Monteiro, M. M. M. Bilek, M. Keidar, E. Oks, and A. Vizir, *Rev. Sci. Instrum.* **71**, 1086 (2000).
- ²⁰M. Keidar, O. R. Monteiro, A. Anders, and I. D. Boyd, *Appl. Phys. Lett.* **81**, 1183 (2002).
- ²¹I. Levchenko, A. Voloshko, M. Keidar, and I. I. Beilis, *IEEE Trans. Plasma Sci.* **31**, 137 (2003).
- ²²A. Anders, S. Anders, and I. G. Brown, *Plasma Sources Sci. Technol.* **4**, 01 (1995).
- ²³B. Juttner, *J. Phys. D* **28**, 516 (1995).